Investigation of Broadband Radiative Flux Changes Due to Increases in Droplet Number Concentrations

L. Oreopoulos and S. Platnick
Joint Center for Earth Systems Technology
University of Maryland Baltimore County
Baltimore, Maryland

S. Platnick and L. Oreopoulos
Laboratory for Atmospheres
National Aeronautics and Space Administration/Goddard Space Flight Center
Greenbelt, Maryland

Introduction

Studying the modification of cloud microphysical and optical properties by anthropogenic aerosols (i.e., the "indirect" or "Twomey" effect) is a major component of Atmospheric Radiation Measurement (ARM's) Program's research effort (see the ARM Science Plan available at http://www.arm.gov/publications/programdocs/doe-er-arm-0402.pdf). While ARM's modeling activities and surface-based observations aiming at elucidating the physical mechanisms of aerosol-induced cloud radiative effects are of great value, satellite observations have a unique role to play. But even with satellites data, the challenges in determining actual cloud changes are many, and originate mainly from the difficulties in trying to quantify a partial derivative (i.e., a temporal change in cloud properties due only to changes in aerosol amount and type, while all relevant dynamic/thermodynamic quantities remain fixed). Rather than confronting the formidable task of assessing the partial derivative of cloud properties in a particular place and time, we have adopted an alternative approach where satellite retrievals are used to estimate the radiative response or sensitivity to some specified change in cloud droplet number. Global spatial and temporal distributions of the albedo sensitivity can be used to estimate the range of future radiative flux responses, as well as provide an additional constraint in indirect effect modeling studies. Our method is thus an attempt to quantify the impact of well-posed hypothetical scenarios of cloud droplet concentration changes, and does not address cloud albedo modifications that may have already occurred.

In this regard, it is appropriate to revisit the previously introduced concept of "cloud albedo susceptibility," a sensitivity parameter given by the cloud albedo change for a differential change in cloud droplet number concentration under constant liquid water content conditions. The new work presented here, broadens the study of cloud susceptibility that has so far been limited to narrowband

cloud albedo changes in the visible part of the spectrum. In order to address broadband (BB) albedo susceptibility, in addition to changes in cloud extinction stemming from modified effective droplet sizes, perturbations in the cloud droplet asymmetry parameter and single scattering albedo have to be taken into account as well.

All the above issues are highlighted below with satellite-based (moderate-resolution imaging spectroradiometer [MODIS]) susceptibility calculations for liquid clouds. We also present an alternative method to calculate albedo perturbations based on relative (rather than fixed) changes in cloud droplet number density.

Droplet Number Perturbations and Susceptibility Calculations

The theory of albedo changes due to perturbations in cloud droplet number density was presented by Twomey (1974) and Platnick and Twomey 1994 (hereafter, PT94). They defined the cloud albedo susceptibility as the change in albedo R resulting from a differential change in cloud droplet number density N

$$\frac{dR_\lambda(\tau_\lambda, g_\lambda, \tilde{\omega}_\lambda)}{dN} = \frac{\partial R_\lambda}{\partial \tau_\lambda}\frac{d\tau_\lambda}{dr_e}\frac{dr_e}{dN} + \frac{\partial R_\lambda}{\partial g_\lambda}\frac{dg_\lambda}{dr_e}\frac{dr_e}{dN} + \frac{\partial R_\lambda}{\partial \tilde{\omega}_\lambda}\frac{d\tilde{\omega}_\lambda}{dr_e}\frac{dr_e}{dN} \tag{1}$$

where

$$r_e = \frac{\int r^3 n(r) dr}{\int r^2 n(r) dr}$$

is the effective radius of the droplet size distribution $n(r)$. The other symbols in Eq. (1) are: λ for wavelength, τ for cloud optical thickness, $\tilde{\omega}$ for droplet single scattering albedo and g for droplet asymmetry factor.

Under the assumption of constant liquid water content (w) the derivative dr_e/dN is negative. The derivatives $d\tau_\lambda/dr_e$ and $d\tilde{\omega}_\lambda / dr_e$ are negative, while $dg_\lambda/dr_e > 0$. Given that albedo increases with τ_λ and $\tilde{\omega}_\lambda$, while it decreases with g_λ, all three terms in the right hand side (RHS) of Eq. (1) are positive and express the contribution of extinction, g and $\tilde{\omega}_\lambda$ to the increase in albedo when N increases for fixed w, but the first term is dominant. The common derivative dr_e/dN is specified as follows. Under the assumption that r_e is related to the volume radius r_υ defined as

$$r_\upsilon = \frac{\int r^3 n(r) dr}{\int n(r) dr}$$

via $r_\upsilon = k r_e$ (k is constant with value ~0.9), the droplet number density N is given by:

$$N = \frac{3w}{4\rho_w \pi k^3 r_e^3} \tag{2}$$

where ρ_w is the water density. If w remains constant, a perturbation $\Delta N>0$ yields a smaller r_e. From Eq. (2), the perturbed effective radius r_e' is given by:

$$r_e' = r_e\left(\frac{N}{N+\Delta N}\right)^{1/3} = r_e\left(\frac{1}{1+\frac{\Delta N}{N}}\right)^{1/3} \Rightarrow \frac{\Delta r_e}{r_e} \approx -\frac{1}{3}\frac{\Delta N}{N} \tag{3}$$

With these assumptions, Platnick and Twomey (1994) showed that the dominant first term on the RHS of Eq. (1) can be expressed as:

$$\frac{\partial R_\lambda}{\partial \tau_\lambda}\frac{d\tau_\lambda}{dr_e}\frac{dr_e}{dN} \approx \frac{4\pi}{9w}\tau_\lambda \frac{\partial R_\lambda}{\partial \tau_\lambda} r_e^3 \tag{4}$$

To obtain all terms in Eq. (1) we can approximate the derivative dr_e/dN with a perturbation ΔN=1 cm^{-3}. Then Eq. (3) indicates that we need to know (or assume) the value of N, or alternatively because of Eq. (2), to know or assume a value of w. The results shown here are for a value w=0.3 gm^{-3}, but susceptibility for other values of w can be approximated by adjusting with a factor w/0.3 because of Eq. (4) for the dominant term. The restriction that w be known can be circumvented by calculating albedo perturbations caused by effective radius perturbations corresponding to assumed a relative changes $\Delta N/N$ in Eq. (3).

The susceptibility and albedo perturbation calculations in this paper were performed with the BB Column Radiation Model (CORAM) used in National Aeronautics and Space Administration-Goddard Large Scale Models (Chou et al. 1998). The model has the capability of calculating flux profiles over the entire solar spectrum (0.2-5 μm) and over the UV-VIS (0.2-0.7 μm) and near infrared (0.7-5 μm) bands separately. It can account for molecular absorption and scattering, aerosol absorption and scattering (neglected here), cloud absorption and scattering (for both the liquid and ice phases), and surface reflection with and without a vegetation canopy. Since our calculations pertain to overcast conditions only, the cloud fraction overlap assumptions of the CORAM are not used. We have modified the original parameterization of cloud single-scattering properties by replacing the original polynomial-

fits with look-up tables that give extinction, $\tilde{\omega}$, and g as function of r_e within the range 3-30 μm. The look-up tables are based on the Hu and Stamnes (1993) values averaged across the four spectral bands of the CORAM following the method of Chou et al. (1998).

Susceptibility and albedo perturbation calculations were carried out with the CORAM for two cases: one where all terms in the RHS of Eq. (1) are accounted for ("all-term" case), and one where only the (much stronger) first term ("one-term" case) is retained. The calculations were performed as follows: The τ value of a (τ, r_e) pair retrieved by MODIS was assumed to represent the optical thickness value of the CORAM's UV-VIS band. From the extinction that corresponds to the MODIS r_e value for that band, the liquid water path W was calculated. The (W, r_e) pair was then used as input to the CORAM for the calculation of the baseline R for the particular solar zenith angle, in the usual way. For "all-term" susceptibility and albedo perturbation calculations, the modified value of r_e (r_e') was estimated from Eq. (3) for ΔN=1 cm^{-3} or $\Delta N/N$=10%, and a new albedo was calculated by the CORAM, again in the usual way. For "one-term susceptibility," r_e' was used to calculate a new value of extinction coefficient, but the unperturbed value r_e was used for the calculation of g and $\tilde{\omega}$. Thus, the estimation of the derivatives in Eq. (1) is done implicitly within the CORAM.

MODIS Data Granule

Figure 1 shows an example of susceptibility calculations for the liquid water clouds of a MODIS granule off the west coast of South America (third panel from left). Susceptibility correlates with r_e (second panel) because of the presence of r_e^3 in the dominant susceptibility term (cf. Eq. 2 and Figure 2). The largest values of susceptibility are associated with the less reliable high values of inferred effective radius near cloud edges and in the southwestern portion of the granule where thin broken clouds are prevalent. Figure 3 shows the relative changes of Δr_e and ΔN corresponding to ΔN=1 cm^{-3} and w = 0.3 gm^{-3} when N is derived from Eq. (2). It can be seen that for r_e < 20 μm the relative change in ΔN is below 10%, and that the ratio of relative changes in r_e to relative changes in N is close to 1/3 as predicted from Eq. (3). Figure 4 shows that neglecting the 2nd and 3rd term in the RHS of Eq. (1) results in underestimates of ~20-40% in the BB albedo susceptibility. The underestimate is much smaller (~10%) for wavelengths below 0.7 μm ("UV-VIS") where due to the conservative nature of cloud scattering there is no susceptibility contribution from the third term.

The albedo perturbation shown in the fourth panel is based on a fixed relative change in N (10%) yielding relative r_e changes given by Eq. (3), and does not require an assumed value of w. The albedo perturbation field looks completely different from the susceptibility field, exhibiting its highest values at low to moderate values of r_e and moderate values of τ. The differences resulting for the two different ways of perturbing N underlines the importance of studying the exact nature of the cloud-aerosol interactions. Will pollution increase cloud condensation nuclei concentrations by some absolute number or by some fixed factor and will the clouds respond by specific absolute or relative changes in N? The effect on a cloud that has an initial droplet concentration of, e.g., 10 cm^{-3} can be very different than for a

cloud with the same w, but N=100 cm^{-3}. Moreover, the values of albedo perturbation are highly sensitive to the exact value of $\Delta N/N$, so that larger albedo perturbations will result from larger relative changes of N.

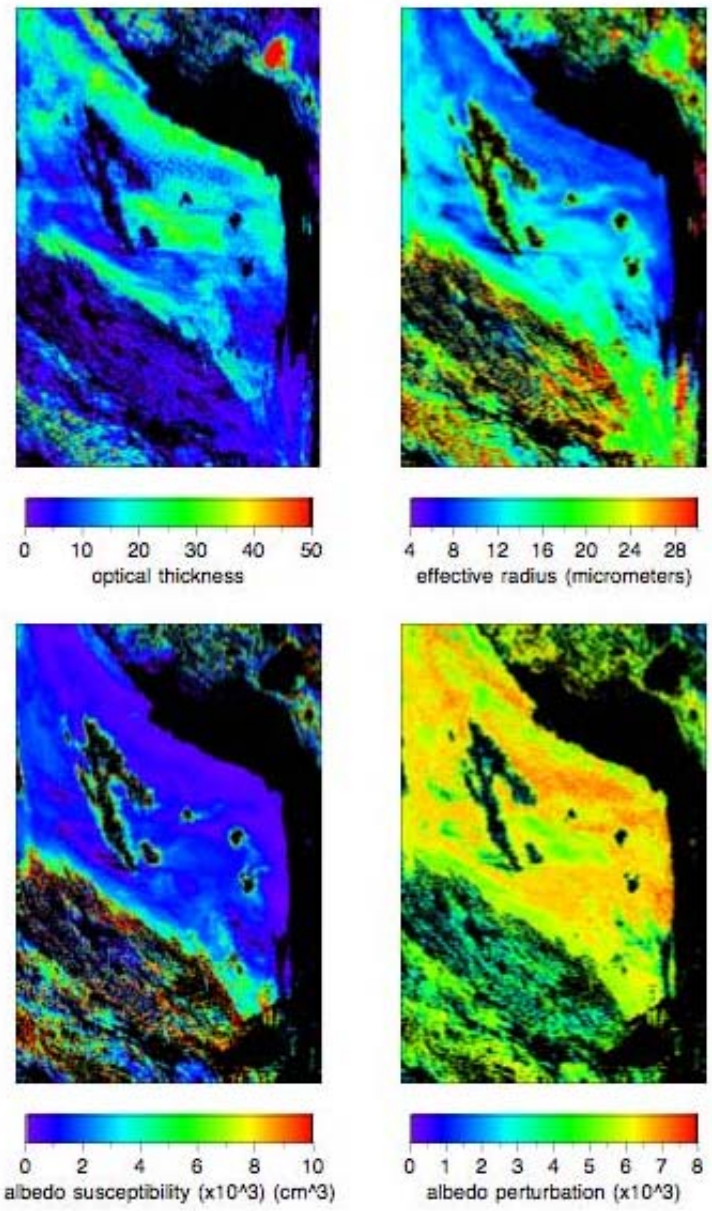

Figure 1. Cloud properties, susceptibility, and albedo perturbation at 5 km resolution for a MODIS data granule observed on July 18, 2001 in the vicinity of the Peruvian coast. Clockwise from top left: cloud optical thickness; cloud effective radius; albedo perturbation for $\Delta N/N$=10%; BB all-term albedo susceptibility for w=0.3 gm^{-3}. Atmospheric and surface albedo effects are taken into account in the susceptibility and albedo perturbation calculations.

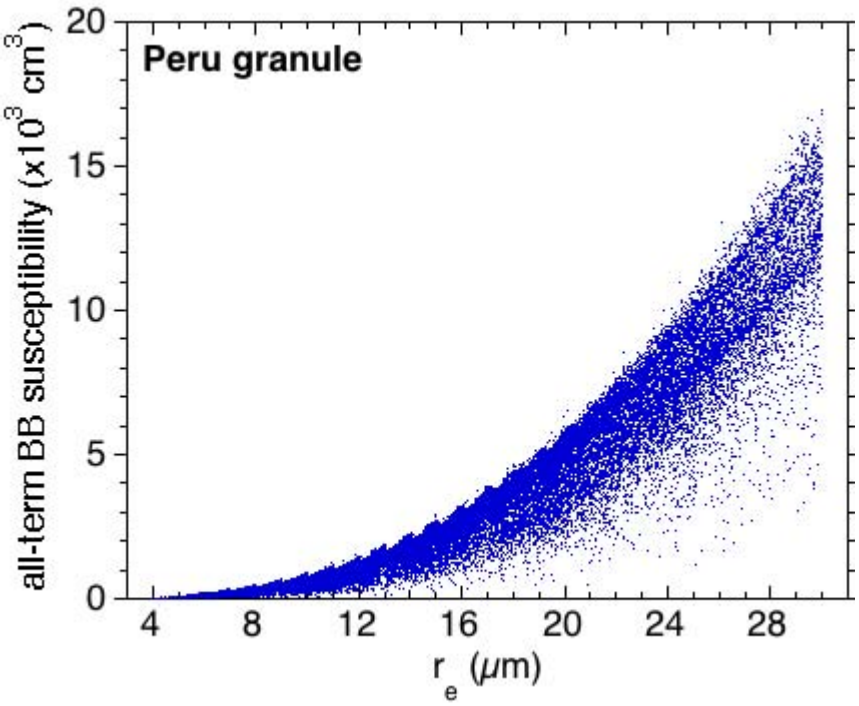

Figure 2. All-term susceptibility dependence on r_e for the MODIS Peru granule. The cubic dependence on r_e of the first term in Eq. (1), as given by Eq. (4), can be seen.

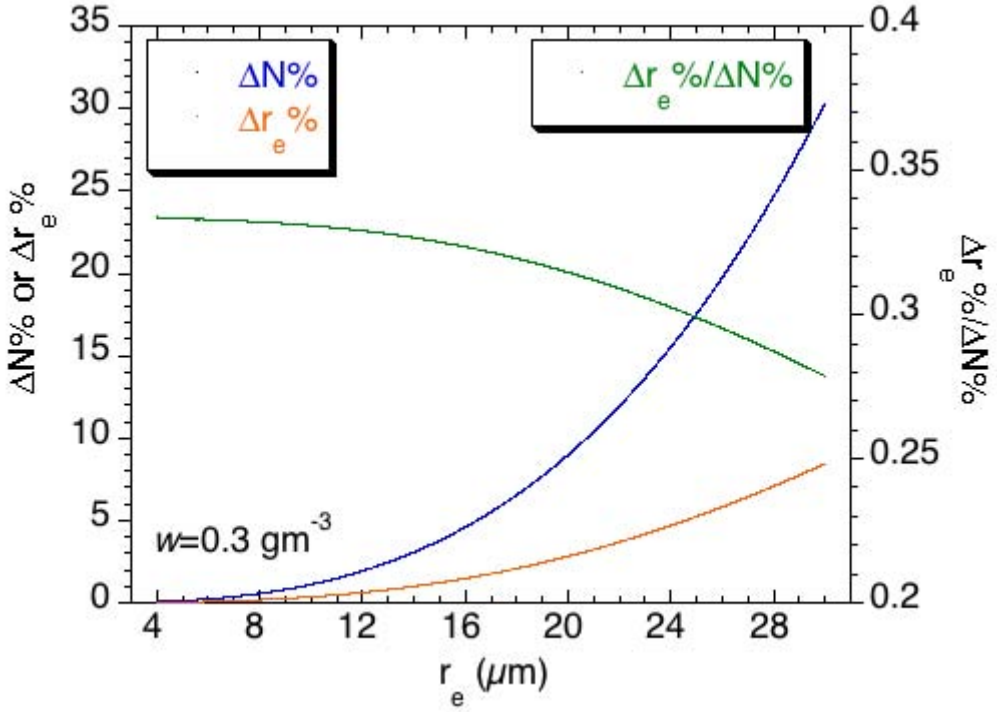

Figure 3. Relative change in N and r_e, as well as their ratio for w=0.3 gm^{-3} and ΔN=1 cm^{-3} in the Peru granule. The ratio is close to 1/3 as predicted by Eq. (3)

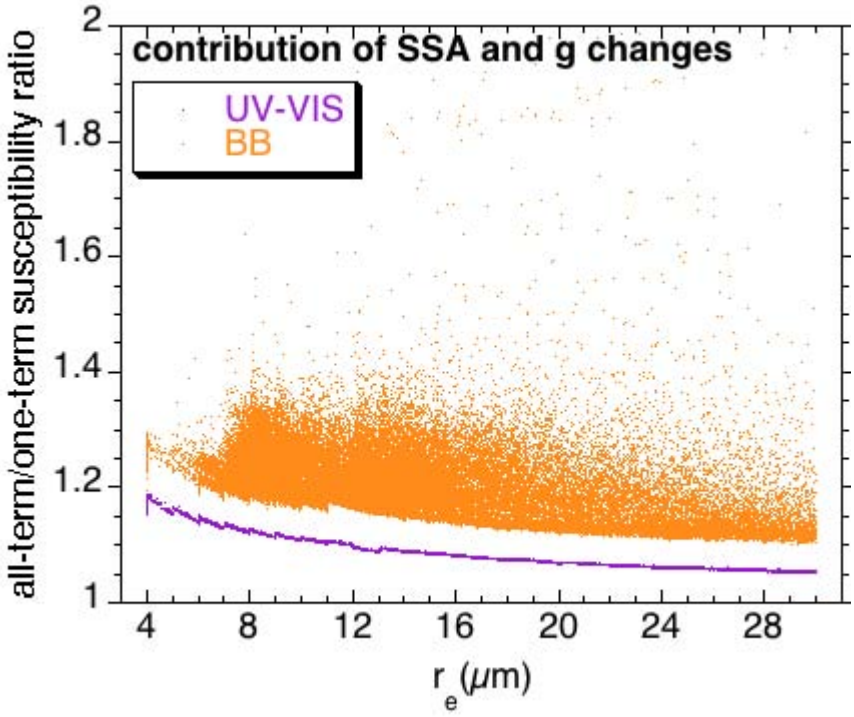

Figure 4. Ratio of Eq. (1) over its first term for BB calculations and calculations between 0.2 and 0.7 μm (UV-VIS) for the Peru granule. No atmospheric or surface effects are accounted for in this plot.

MODIS Level-3

For practical reasons, global distributions of susceptibility and albedo perturbations for liquid clouds are best calculated from MODIS Level-3 data. A number of options are available to perform the actual calculations, and the most accurate (albeit more arduous) is to use the joint histograms of liquid water τ and r_e that are available daily for each 1° x 1° gridpoint. The monthly-averaged results (weighted by liquid water cloud fraction) of these calculations are shown in Figure 5. Surface albedo and atmospheric absorption are accounted for in these calculations. Susceptibility is in general negatively correlated with albedo while the opposite is true for albedo perturbation arising from fixed relative changes of $\Delta N/N$. The latter, however, is not true where the combined albedo of the surface and atmospheric column is already large, like in the northernmost latitudes and Antarctica. This stresses the important point that the exact geographical distribution of the combined τ-r_e variations in unperturbed clouds is a major factor determining the ultimate radiative impact of polluted clouds. Instances where the impact of high cloud susceptibilities is radiatively diminished can be found in locations with high surface albedo or (to a lesser degree) high humidity, and in regions of systematically low illuminations where not only is the cloud albedo already high, but the amount of incident solar radiation is small.

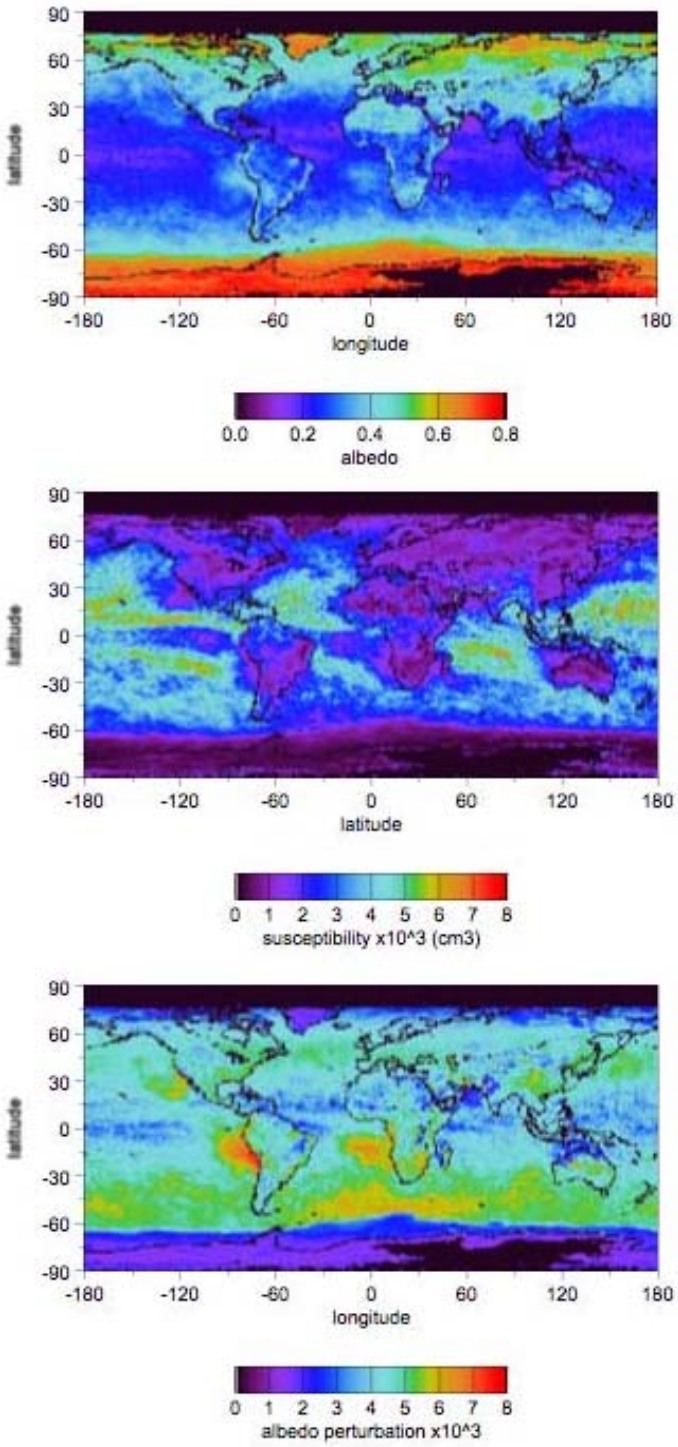

Figure 5. Cloud albedo (top), susceptibility (middle) and albedo perturbation (bottom) from MODIS Level-3 daily data (Collection 4, D3) for October 2003. Atmospheric (but no-aerosol) and surface albedo effects are accounted for. Susceptibility is for w=0.3 gm^{-3} and albedo perturbation is for $\Delta N/N$=10%.

Relevance to Indirect Effect Studies

We have presented the concept of cloud albedo susceptibility which describes potential albedo changes due to cloud microphysical modifications in aerosol-laden atmospheres (the so-called "first indirect aerosol effect") and demonstrated how susceptibility can be calculated by pairing satellite observations with a shortwave radiative transfer algorithm. We have extended previous work on narrowband visible susceptibility to broadband albedo susceptibility that accounts not only for extinction, but for all optical property perturbations. Moreover, the susceptibility now refers to the entire atmosphere column-surface system instead of just the cloud itself.

An important issue that remains to be resolved is whether fixed absolute or relative changes in droplet number concentration are more realistic in climate change scenarios. Experiments with Large Eddy Simulation models that are capable of explicitly resolving cloud condensation nuclei activation and cloud microphysics may provide some clues, but in the meantime we will continue to study the radiative consequences of both scenarios. Our ultimate goal is to use MODIS datasets to build a global susceptibility and albedo perturbation climatology (including ice clouds) and investigate possible correlations with global aerosol distributions. We hope that our study will be useful for (1) obtaining a range of observationally-based estimates of the indirect effect; (2) indirect effect model validation; (3) exploring the inherent sensitivity of a GCM cloud scheme to conditions of enhanced could condensation nuclei concentrations.

Author Contacts

Lazaros Oreopoulos, (301) 614-6128, lazaros@climate.gsfc.nasa.gov

Steven Platnick, (301) 614-6243, steven.platnick@nasa.gov

References

Chou, M-D, MJ Suarez, C-H Ho, MM-H Yan, and K-T Lee. 1998. "Parameterizations for cloud overlapping and shortwave single-scattering properties for use in general circulation and cloud ensemble models." *Journal of Climate* 11:202-214.

Hu, YX, and K Stamnes. 1993. "An accurate parameterization of the radiative properties of water clouds suitable for use in climate models." *Journal of Climate* 6:728–742.

Platnick, S, and S Twomey. 1994. "Determining the susceptibility of cloud albedo to changes in droplet concentration with the advanced very high resolution radiometer." *Journal of Applied Meteorology* 33:334-347.

Twomey, S. 1974. "Pollution and the planetary albedo." *Atmospheric Environment* 8:1251-1256.